CONSTRUCTAL DESIGN OF AN ONSHORE OVERTOPPING DEVICE IN REAL SCALE FOR TWO DIFFERENT OCEAN WAVE PERIODS AND DIFFERENT AREAS OF THE RAMP

Jaifer Corrêa Martins

Dante Vinícius Eloy Barbosa

Marcelo Moraes Goulart

jaifercm@gmail.com

dante_barbosa@yahoo.com.br

moraesgoulart@yahoo.com.br

Universidade Federal do Rio Grande

Avenida Itália, km 8, CP.474, Rio Grande, RS, Brasil

Luiz Alberto Oliveira Rocha

luizrocha@mecanica.ufrgs.br

Universidade Federal do Rio Grande do Sul

CEP 90050-170, Porto Alegre, RS, Brasil

Mateus das Neves Gomes

Mateus.gomes@ifpr.edu.br

Instituto Federal do Paraná, Campus Paranaguá

CEP 83215-750, Paranaguá, PR, Brasil

Jeferson Avila Souza

Liércio André Isoldi

Elizaldo Domingues dos Santos

elizaldosantos@furg.br

liercioisoldi@furg.br

jasouza@furg.br

Universidade Federal do Rio Grande

Avenida Itália, km 8, CP.474, Rio Grande, RS, Brasil

Abstract. *The study about technologies and operational principles of devices to convert wave energy into electrical one (WEC) has increased significantly. Among the studied WECs it is possible to mention the overtopping device. It is main operational principle consists on a ramp which guides the incoming waves into a reservoir raised slightly above the sea level. The accumulated water in the reservoir flows through a low head turbine generating electricity. In the present work it is performed a numerical study concerned with the effect of ramp geometry over the performance of an onshore overtopping device in real scale by means of Constructal Design. The purpose of this study is to evaluate the effect of the ramp volume fraction (φ) and the ratio between the height and length of the ramp (H_1/L_1) over the amount of water that enters into device reservoir for two different ocean wave periods (T = 5.0 s and 7.5 s). All cases are performed for one specific distance from the bottom of the tank to the bottom of device of S = 5.0 m. Moreover, three different ramp volume fractions are investigated: φ = 0.006, φ = 0.012 and φ = 0.024. For all studied cases the conservation equations of mass, momentum and one equation for the transport of volumetric fraction are solved with the finite volume method (FVM). To tackle with water-air mixture, the multiphase model Volume of Fluid (VOF) is used. Results showed that Constructal Design allowed an improvement of the shape of ramp. In general, the optimal shapes performed several times better than the worst ones. Results also depicted that the mass of water stored in the reservoir increased with the increase of wave period from T = 5.0 s to T = 7.5 s.*

Keywords: *Constructal Design, Overtopping Device, Geometric Optimization, Numerical Study*

1 INTRODUCTION

The main physical operational principle of overtopping device has not been widely studied as other kind of devices, one example of this fact can be seen in the amount of discussion for each operational principle in review literature (Falcão, 2010; Zabihian and Fung, 2011). Among the works concerned with overtopping devices, efforts have been devoted in the development of experimental studies for evaluation of building parameters of device (Kofoed et al., 2006; Margheritini et al., 2009). More recently, some studies have been performed into numerical framework with the purpose to improve the comprehension about the fluid flow phenomenology and to investigate the geometrical parameters of device (Beels et al., 2010; Rocha et al., 2013; Nam et al., 2008; Margheritini et al., 2012; Jin et al., 2012). The main operational principle of an overtopping device consists on the water accumulation into a reservoir raised slightly above the sea level. The wave water overtops the inclined ramp and enters into reservoir. The accumulated water returns to the sea passing through low head hydraulic turbines generating electricity. Figure 1 depicts a schematic sketch with the main operational principle of this device.

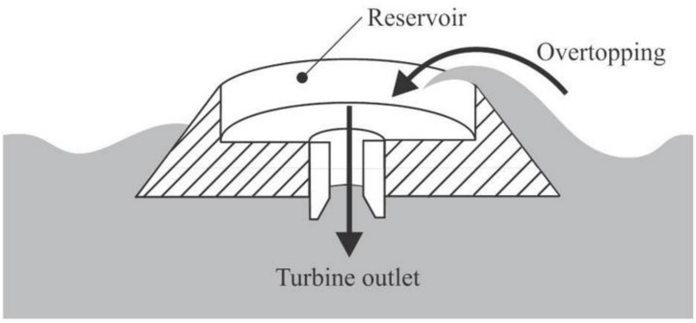

Figure 1. Illustration of physical main operational principle of overtopping device.

Concerning the experimental studies about the overtopping device, Kofoed *et al*. (2006) performed extensive tests of a prototype with reduced scale of 1:50 inside a wave tank. Afterwards, the authors build a new prototype in reduced scale with 1:4.5 of a Wave Dragon. This device was evaluated during three years being monitored parameters as power, wave climate, forces in mooring lines and structure tension. The purpose was to determine the design for the structure, as well as, development of a plain to implement an unit for generation of 4 MW. Other important study is presented in Margheritini *et al.* (2009) which analyzed a device named Sea Slot-cone Generator (SSG) which consists on a device with multiple ramps. The pilot plant is an onshore module in real scale with three different ramps capturing waves of different heights.

Into the numerical framework, Liu *et al.* (2008) and Nam *et al*. (2008) evaluated an overtopping device. In the first, was employed the methodology Volume of Fluid (VOF) for the modeling of water-air flow. The conservation equations were solved with the Finite Volume Method (FVM), with FLUENT^{TM} software. In the second study, the simulations were performed with commercial software FLOW3D, based on the Finite Difference Method (FDM). In this work it was performed two and three-dimensional simulations with the aim to evaluate the best geometry for accumulation of water inside the device reservoir.

Iahnke (2010) employed the Constructal Design, but was not performed by the imposition of constant area, to evaluated the ramp inclination of an overtopping device for a two-dimensional flow. The best performance was obtained for a ramp with an angle of 30º. In the same year, Bells *et al.* (2010) used a numerical model called mildslope to solve the transient flow in a farm of Wave Dragon devices. For the evaluation of the devices arrangement it was tested different distances between the different equipment. As a result, the farm with five devices installed with a staggered arrangement is more efficient due to the best utilization of space and without significant interference of one converter in the others.

Jin *et al.* (2012) performed a similar study to that in Nam *et al.* (2008), where it was employed the software FLUENT™ instead the FLOW3D. In this work, it was performed a comparison between an overtopping device with and without fins over the ramp. The geometrical evaluation was neither performed into the Constructal Design framework.

Dos Santos *et al.* (2014) performed a numerical study to determine the influence of geometry on the performance of an offshore overtopping device in laboratory scale to three different depths for: h/λ = 0.3, 0.5 and 0.62 using the Constructal Design. In this study, the conservation equations of mass, momentum and one equation for the transport of volumetric fraction are solved with the Finite Volume Method (FVM). For the solution of the water-air interface is used multiphase model Volume of Fluid (VOF). The results showed that the optimal ratio between height and length of the ramp, $(H_1/L_1)_o$, showed a strong dependence of the relative depth, indicating the absence of an universal geometry leading to the best performance of a device for overtopping different wave conditions.

Recently, Goulart *et al.*(2015) performed a 2D numerical study about the effect of the ramp geometry on the performance of an onshore overtopping device in real scale employing Constructal Design. It is evaluated the effect of ratio between height and length of the ramp (H_1/L_1) over the mass of water (m) entering into the reservoir for two different depths (S = 5.0 m and 6.0 m). A computational model based on the FVM and VOF to tackle with the mixture of water/air was employed.

The present work aims to perform a numerical study about the geometry of an onshore overtopping device ramp in real scale which leads to the highest fluid dynamic performance. The shape of overtopping ramp is varied by means of Constructal Design (Bejan, 2000; Bejan and Lorente, 2008). More precisely, it is evaluated the influence of the ratio between height and length of the ramp (H_1/L_1) over the amount of mass entering into the reservoir for two different wave periods (T = 5.0 s and 7.5 s). Moreover, three different ramp volume fractions are investigated: φ = 0.006, φ = 0.012 and φ = 0.024. All cases are performed for one specific distance from the bottom of the tank to the bottom of device of S = 5.0 m.

2 MATEMATICAL MODELING

The physical problem analyzed is a two-dimensional overtopping device placed in a wave tank, as shown in Fig. 2. The third dimension Y is perpendicular to the plane of the figure. The wave motion is generated by imposing a velocity profile at the left surface of the tank. The objective of the analysis is to determine the ideal geometry (H_1/L_1) leading to higher amount of water entering in the reservoir. The degree of freedom H_1/L_1 is optimized for a flow with depth h = 10.0 m, wavelengths of λ = 36.6 m and 65.4 m (relative depths of h/λ = 0.27 and 0.15), wave height of H = 1.0 m and the periods T = 5.0 s and 7.5 s. It is also maintained fixed the following parameters: H_T = 20.0m (height of the tank), L_T = 327.0 m (length of the tank) which leads to a ratio of (H_T/L_T = 0.0612). In addition, it will be considered a reservoir with length of L_R = 20.0 m and distance between the device and the tank bottom of S = 5.0 m. For this value of S it have been simulated several ratios of H_1/L_1 for two different ocean wave periods (T = 5.0 s and 7.5 s) and three different fraction areas of the ramp ($\varphi = A_r/A_T$ = 0.006, 0.012 and 0.024). According to Constructal Design, the optimization problem is subjected to two constraints, i. e., the total area of the surge tank restriction

$$A_T = H_T L_T \tag{1}$$

and the area of the ramp

$$A_r = \frac{H_1 L_1}{2} \tag{2}$$

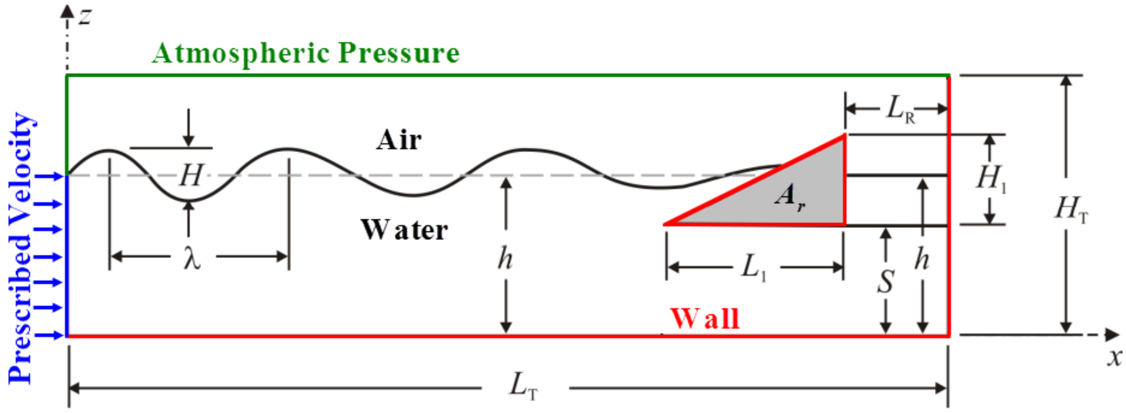

Figure 2. Computational domain of the overtopping device in real scale studied in the present work.

A function of volume (area) fraction of the device can be defined as

$$\varphi = \frac{A_r}{A_T} \tag{3}$$

It is also being considered as a restriction of the problem $(S + H_1) > (h + H/2)$ so that the crest of the wave does not exceed the maximum height of the device.

The area of the ramp (A_r) was defined considering a device in real scale. Thus, it is adopted the value used to build the OWC device ramp located on the Pico Island in Portugal. To define the height and length of the tank (H_T and L_T, respectively) it is considered a depth of water layer, h = 10 m, and parameters of waves commonly found in the south of Brazil (Rio Grande city). In order to avoid interaction of wave flow with the upper region of the tank, its height is defined as H_T = 20.0 m. With the purpose to avoid wave reflection and allow the evaluation of the highest possible time interval of overtopping, the tank is constructed with a length five times higher than the highest wavelength (λ = 65.4 m), i.e., L_T = 327 m. For the other wave climate (T = 5.0 s) the tank is maintained with the same dimensions.

Concerning the optimization process, it is divided into two steps as shown in Fig. 3, for the two different ocean wave periods (T = 5.0 s and 7.5 s). In the first step, the geometry is optimized by variation of the ratio H_1/L_1 and keeping fixed the remaining parameters, in this case the submersion S (S = 5.0 m) and ramp fraction area (φ = 0.006). The maximum value found for the mass of water entering the reservoir is called the mass of water entering into the reservoir once maximized, m_m, and the corresponding ratio H_1/L_1 is referred to the once optimized ratio of H_1/L_1, $(H_1/L_1)_o$. In a second step, the same process is repeated for other values of ramp fraction area (φ = 0.012 and 0.024). For the present study, an amount of 48 simulations (half for each ocean wave period) were performed with the following distribution: φ = 0.006 (16 cases), φ = 0.012 (16 cases) and φ = 0.024 (16 cases).

2.1 The Multiphase Volume of Fluid (VOF) Model

The conservation equation of mass for the mixture of air and water in an isothermal, laminar and incompressible flow is given by (dos Santos et al., 2014):

$$\frac{\partial \rho}{\partial t} + \nabla.(\rho \vec{v}) = 0 \tag{4}$$

where ρ is the density of the mixture (kg/m³) and $\vec{v}$ is the flow velocity vector (m/s).

The momentum equation for the mixture is given by:

$$\frac{\partial \rho}{\partial t}(\rho \vec{v}) + \nabla.(\rho \vec{v}\vec{v}) = \nabla p + \nabla.(\bar{\bar{\tau}}) + \rho \vec{g} + \vec{F} \tag{5}$$

where p is the pressure (N/m ²), $\rho\vec{v}$ and $\vec{F}$ are, respectively, the buoyancy and external body forces (N/m³), which is null in the present work, and $\bar{\bar{\tau}}$ is the rate of deformation tensor (N/m²).

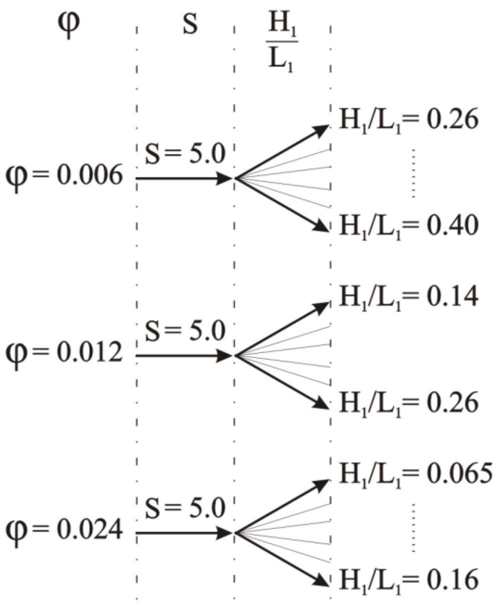

Figure 3. Illustration of the optimization process applied to overtopping device with different device fraction areas.

To tackle with the mixture of air and water and to evaluate their interaction with the device, the method Volume of fluid (VOF) has been employed. The VOF is used to model multiphase fluid flows with two or more phases. In this model, the phases are immiscible, i. e., the volume of one phase may not be occupied by another phase (Lv et al., 2011).

In the simulations of this study, it is considered two different phases: air and water. Therefore, the concept of volume fraction (α_q) is used to represent the two phases in a volume control. In this model, the sum of the volume fractions within a control volume must be unitary ($0 \leq \alpha_q \leq 1$). Consequently, if $\alpha_{water} = 0$, the volume control is empty of water and full of air ($\alpha_{air} = 1$). If the fluid is a mixture of air and water, one phase is the complement of the other, $\alpha_{air} = 1 - \alpha_{water}$. Thus, an additional transport equation for the volume fractions is required (dos Santos et al., 2014; Lv et al., 2011):

$$\frac{\partial(\rho\alpha_{water})}{\partial t} + \nabla.(\rho\alpha_{water}\ \vec{v}) = 0 \tag{6}$$

It is noteworthy that the conservation equations of mass and momentum are solved for the mixture. Therefore, it is necessary to obtain the density and viscosity values for the mixture, which can be written by:

$$\rho = \alpha_{water}\ \rho_{water} + \alpha_{air}\ \rho_{air} \tag{7}$$

$$\mu = \alpha_{water}\ \rho_{water} + \alpha_{air}\ \rho_{air} \tag{8}$$

Regarding the wave generation, a velocity profile is imposed at the left side surface of Fig. 2 and simulates the behavior of a wavemaker (Horko, 2007). The velocity components in the wave propagation direction (x) and vertical (z) imposed in the left surface of the domain are based on Stokes of 2nd order theory and given respectively by (Chakrabarti, 2005):

$$u(x,z) = \frac{Hgk}{2\sigma}\frac{\cosh k(h+z)}{\cosh kh}\cos(kx-\sigma t) + \frac{3H^2\sigma k}{16}\frac{\cosh 2k(h+z)}{\sinh^4 kh}\cos 2(kx-\sigma t) \tag{9}$$

$$w(x,z) = \frac{Hgk}{2\sigma}\frac{\sinh k(h+z)}{\cosh kh}\sin(kx-\sigma t) + \frac{3H^2\sigma k}{16}\frac{\sinh 2k(h+z)}{\sinh^4 kh}\sin 2(kx-\sigma t) \tag{10}$$

where H is the wave height (m), k is the wave number given by $k = 2\pi/\lambda$ (m^{-1}), h is the water depth (m), T is the wave period (s), $\sigma = 2\pi/T$ is the frequency (rad/s) and t is the time (s).

For the other boundary conditions, the superior region of left side surface and the superior surface is considered at atmospheric pressure P_{abs} = 101.3 kPa (dashed lines in Fig. 2). In the lower and right surfaces, as well as, in the overtopping device surfaces it is imposed a non-slip condition and impermeability ($u = w = 0$ m/s). Regarding the initial conditions, it is considered that the fluid is at rest and the water has a depth of h = 10.0 m.

3 NUMERICAL PROCEDURES

In present work it is employed the Finite Volume Method (FVM) (Patankar, 1980; Versteeg *et al.*, 2007) for numerical solution of conservation equations of mass, momentum and volume fraction. More precisely it is used the CFD commercial package FLUENT™ (FLUENT, 2007). For the interaction between air, water and device it is employed the multiphase model Volume of Fluid (VOF) (Liu *et al.*, 2008; Lv *et al.*, 2011).

The pressure based solver has been employed for all simulations. First order advection scheme Upwind and PRESTO (Pressure Staggering Option) for the spatial discretization of the advective term and pressure in the momentum equation, respectively, have been used. The pressure-velocity coupling was performed with PISO algorithm (Versteeg and Malalasekera, 2007). The surface of wave flow is determined by the use of Geo-reconstruction method. In addition, sub-relaxation factors of 0.3 and 0.7 were imposed for the conservation equations of mass and momentum, respectively. The solutions obtained here were considered converged when the residual of the conservation equations of mass and momentum in the x and z directions were lower than 10^{-6}.

All simulations were performed using a computer with two dual-core Intel processors clocked at 2.67 GHz and 8 GB of RAM. It is used Message Passing Interface (MPI) for parallelization. The processing time for each simulation was approximately 1.44×10^5 s (40 h).

The discretization of the domain in rectangular finite volumes was performed. As can be seen in Fig. 4, the highest refinement is performed in device surfaces and free surface of wave where the highest velocity gradients are presented. In the study of Gomes et al. (2012) it is presented a theoretical recommendation about the number of finite elements employed along the domain which is adopted in the present study. In this sense, a grid with nearly 120,000 rectangular finite volumes are generated (Fig. 4).

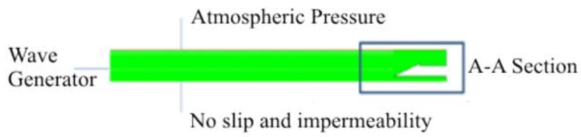

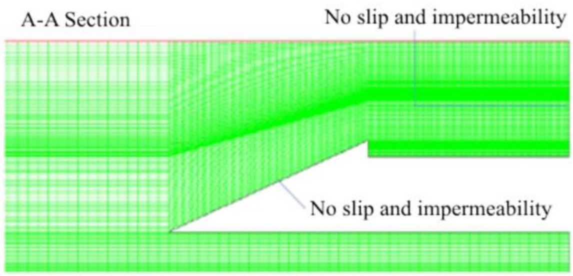

a) **b)**

Figure 4. Spatial discretization applied to the onshore real scale overtopping device

After the definition of the spatial discretization used, it was performed a time step independence study for the transient problem and time-step influence over the height of the free surface wave, Fig. 5 (a). The independent solution was verified with analytical results of Chakrabarti (2005), Fig. 5 (b). In the first study, the height of the free surface wave was obtained for 4 different time steps: $\Delta t = 5.0 \times 10^{-3}$ s, $\Delta t = 1.0 \times 10^{-2}$ s, $\Delta t = 2.0 \times 10^{-2}$ s and $\Delta t = 4.0 \times 10^{-2}$ s. In all simulations the final time is $t_f = 100.0$ s. Figure 5 (a) shows a good agreement between the results for the various studied time steps, with the exception case with com $\Delta t = 4.0 \times 10^{-2}$ s where the predicted wave has differences in time and space in comparison with the others. Consequently, it was adopted in subsequent simulations geometric evaluation with time step of $\Delta t = 2.0 \times 10^{-2}$ s. Concerning the verification process, after the wave stabilization, which occurs at about $t = 15.0$ s, the average deviation obtained between the numerical and analytical solution is 0.1 % and 8.0 % for the water depth and wave height, respectively, showing the good accuracy of the present numerical model.

4 RESULTS AND DISCUSSION

The optimization process consists on the evaluation of total mass of water entering into reservoir for three different ratios of H_1/L_1, for two different ocean wave periods. Figure 6 presents the effect of the ratio H_1/L_1 over the total amount of water entering into reservoir along a considered time interval (0.0 s ≤ t ≤ 100.0 s). Results showed that the geometry has a strong influence over the magnitude of mass accumulated in the reservoir. It is worthy to mention that the total amount of mass is taken into account by the integration of mass flow rate of water entering into reservoir along the time interval considered. Results of Figure 6(a and b) showed that the optimal shapes are achieved for the lowest magnitudes of the ratio H_1/L_1 for each value of φ and two different wave periods, i.e., $(H_1/L_1)_o = 0.39$ for $\varphi = 0.006$, $(H_1/L_1)_o = 0.22$ for $\varphi = 0.012$ and $(H_1/L_1)_o = 0.097$ for $\varphi = 0.024$. It can also be noticed that for each evaluated φ, different range of geometry application is noticed, i.e., the range of ratio H_1/L_1 where overtopping occurs. For instance, for $\varphi = 0.006$ the overtopping occurred in the range $0.39 \leq H_1/L_1 \leq 0.53$. For $\varphi = 0.012$, the range of H_1/L_1 decreases to $0.22 \leq H_1/L_1 \leq 0.38$ and for $\varphi = 0.024$ the ranges decreases even more for $0.097 \leq H_1/L_1 \leq 0.22$. Moreover, to the lowest ocean wave period (T = 5.0 s), was a decrease of the total mass of water entering into reservoir. Results presented in Fig. 6 also showed that the highest once maximized amount of mass entering into reservoir is obtained for the lowest device area fraction (φ = 0.006). For this case, the magnitude of m_m = 4440.38 kg is obtained for T = 5.0 s and m_m = 20213.59 kg for T = 7.5 s, which this is nearly 4.5 times higher than the best geometry obtained for T = 5.0 s. In a general sense, results showed that the employment of Constructal Design can result in an improvement of fluid dynamic performance of this kind of renewable energy device.

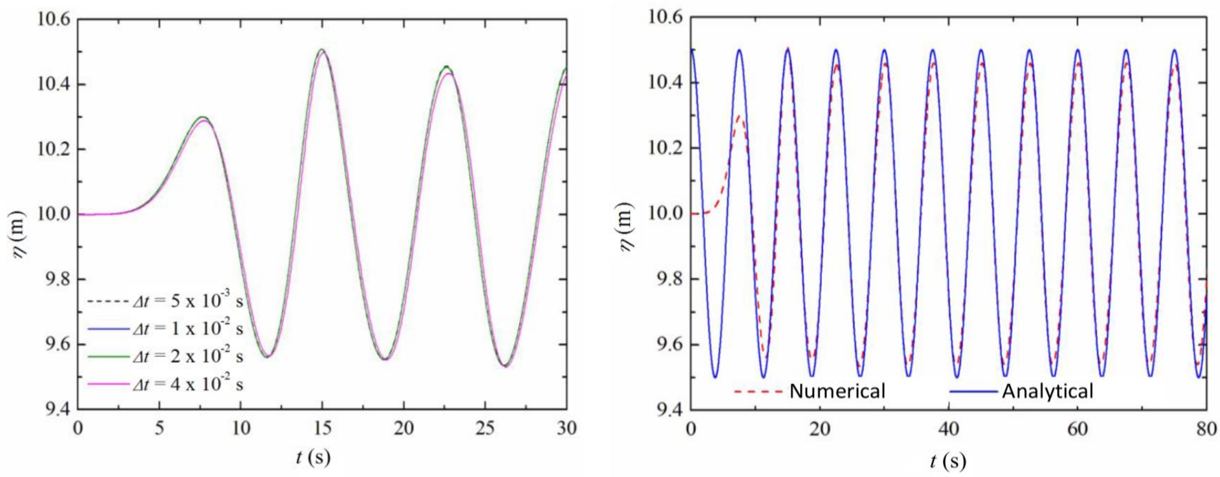

a) **b)**

Figura 5. Numerical evaluation of the employed methodology: a) study of independent time step, b) verification of the numerical solution with the analytical solution presented in Chakrabarti (2005).

Results obtained here showed that the highest amount of mass entering during the evaluated period of time (t = 100.0 s) is achieved for the lowest fraction area of device (φ) and for the highest ocean wave period (T). However, small dimensions for device limit the height dimension of the reservoir. As a consequence, for long periods of time the employment of small devices can became impracticable, once the reservoir does not have capacity enough to accumulate large amount of water. For the studied case, the best recommendation is the building of devices with the lowest possible area fraction and for the lowest ratios of H_1/L_1. For the same construction area, a farm of devices can leads to a better performance than an isolated device. The effect of H_1/L_1 over the mass obtained here is in agreement with those shown in experimental studies of Kofoed (2002), which evaluated an onshore device in laboratory scale.

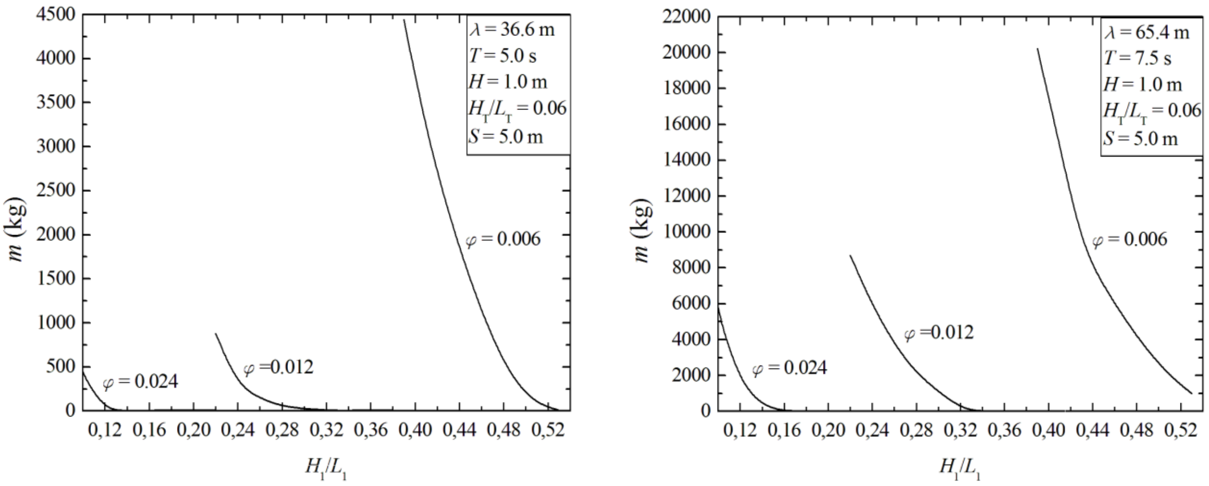

a) **b)**

Figure 6. Effect of the ratio H_1/L_1 over the amount of mass entering into reservoir to present work for a real scale onshore device: a) T = 5.0 s and different values of φ; b) T = 7.5 s and different values of φ.

In order to evaluate the effect of φ and T over the local behavior of wave flow in the overtopping device, Figs. 7(a) and 8(a) illustrate the instantaneous mass flow rate of water in the time interval (0.0 s ≤ t ≤ 100.0 s) for the three optimal shapes achieved for each value of φ. Figures 7(b) and 8(b) depict a restrict time interval to improve the visualization of differences between overtopping peaks showed in Figs. 7(a) and 8(a). In Fig. 8(a), for T = 5.0 s, φ = 0.006 and $(H_1/L_1)_o$ = 0.39 the highest magnitude of m_m = 333.94 kg/s was noticed for t ~ 83.0 s, while for φ = 0.012 and $(H_1/L_1)_o$ = 0.22 the highest magnitude of m_m is nearly 7.0 times lower than that found for the case with φ = 0.006. Moreover, the highest peak for the latter case is noticed at t = 80.0s. For φ = 0.024, the overtopping peaks are almost indistinguishable. It can also be seen that some time periods of overtopping are affected by different geometries. In Fig. 8(a), for T = 7.5 s, φ = 0.006 and $(H_1/L_1)_o$ = 0.39 the highest magnitude of m_m = 679.65 kg/s is noticed for t ~ 66.0 s, while for φ = 0.012 and $(H_1/L_1)_o$ = 0.22 the highest magnitude of m_m is nearly 2.7 times lower than that found for the case with φ = 0.006. For φ = 0.024 the highest magnitude of m_m is nearly 2.9 times lower than φ = 0.006. Moreover, for T = 7.5 s the overtopping peaks are noticed before the cases with T = 5.0 s, which is expected since the wave celerity is higher for waves with T = 7.5 s than waves with T = 5.0 s.

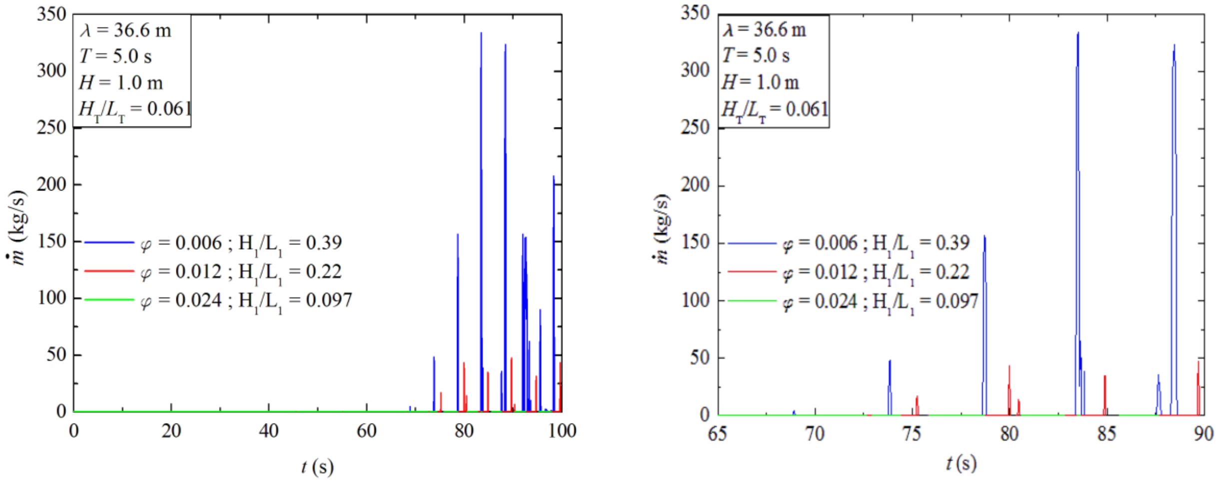

a) **b)**

Figure 7. Instantaneous mass flow rate of water as function of time for T = 5.0 s and three different values of φ: a) time interval of 0.0 s ≤ t ≤ 100.0 s, b) time interval of 65.0 s ≤ t ≤ 90.0 s.

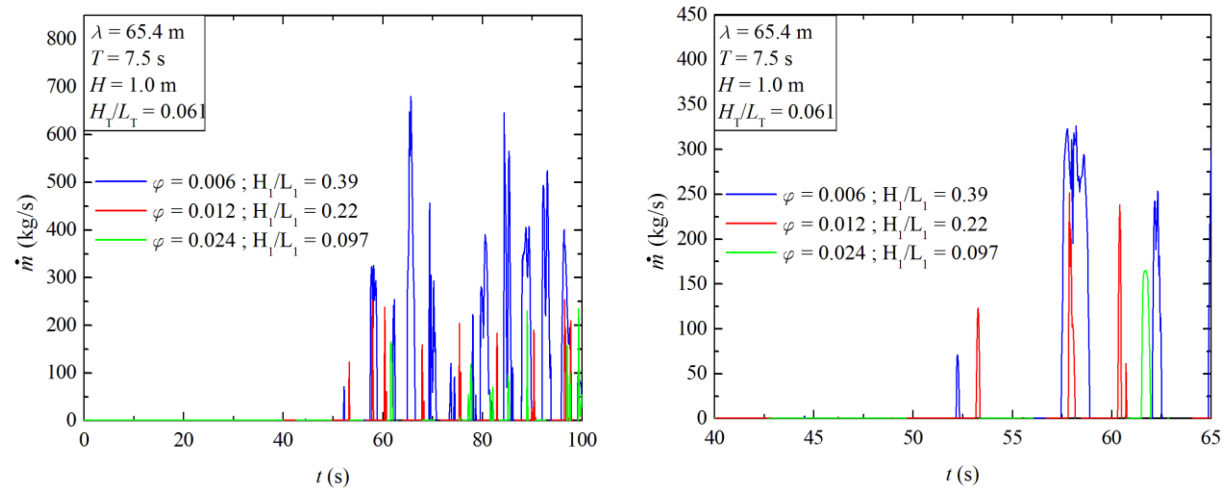

a) **b)**

Figure 8. Instantaneous mass flow rate of water as function of time for T = 7.5 s and three different values of φ: a) time interval of 0.0 s ≤ t ≤ 100.0 s, b) time interval of 40.0 s ≤ t ≤ 65.0 s.

5 CONCLUSION

In present work it was performed a numerical study to evaluate the geometry that conducts to the best fluid dynamic performance of and overtopping device. In this study the device was built in real scale. The analysis was realized by means of Constructal Design for a device with three different area fractions (φ = 0.006, φ = 0.012 and φ = 0.024) and for two different ocean wave periods (T = 5.0 s and T = 7.5 s), evaluating the effect of the ratio H_1/L_1 over the amount of water that enters into the reservoir of the overtopping device. For the studied cases the wave conditions which were employed was: H = 1.0 m, λ = 36.6 m and T =5.0 s ; λ = 65.4 m and T =7.5 s. For this study, it was solved a transient flow of an air-water mixture in laminar regime. The numerical solution of conservation equations of mass, momentum and water volume fraction was obtained by the Finite Volume Method, more precisely with FLUENT™ software (FLUENT, 2007). Volume of Fluid (VOF) method was employed for the treatment of interaction between air and water phases, allowing the generation of regular waves in a wave tank and its interaction with the device. The main purpose here was to evaluate whether the effect of the ratio (H_1/L_1) over the total amount of mass entering into reservoir is similar for different wave parameters, similarly to what was noticed in previous work of Dos Santos et al. (2014) for laboratory offshore device.

Results showed that the highest amount of water entering into the reservoir along the time interval evaluated was obtained for the lowest ratios of H_1/L_1 for the three studied values of φ and for the two different ocean wave periods. Moreover, the highest ratio of H_1/L_1 led to the worst performance of the device. Comparison between the performance obtained with different fraction areas revealed that the highest amount of water were obtained for the lowest fraction area (φ = 0.006) and the highest ocean wave period (T = 7.5 s). Then, it is recommended the building of ramps with small possible areas, since there is sufficient reservoir height for water accumulation inside the device. In a general sense, results showed the importance to evaluate the geometry of this kind of renewable device. Moreover, Constructal Design can be an important tool to guide the geometry evaluation of this kind of problem. Results also indicated that the employment of different values of φ led to similar effect of the ratio H_1/L_1 over the amount of water entering into reservoir. In general, results proved that the fraction area affects the range of applicability of the ratio H_1/L_1. Concerning the wave period, it has a higher influence over the magnitude of water entering into the reservoir and the spreading of time for each overtopping peak. Results also showed a different behavior of the effect of H_1/L_1 over the amount of mass entering into reservoir than that achieved for laboratory offshore device. In other words, results indicate that the solution can be dependent of the placement of device installation or scale of the problem. Future works will be performed to investigate the main reasons for these differences.

6 ACKNOWLEDGEMENTS

The author J. C. Martins thanks CAPES by master science scholarship. The authors J. A. Souza, L. A. O. Rocha, L. A. Isoldi and E. D. dos Santos thank CNPq for research grant and financial support. All authors thank CNPq for financial support.

7 REFERENCES

Beels, C., Troch, P., De Visch, K., Kofoed, J.P., De Backer, G., 2010. Application of the time-dependent mild-slope equations for the simulation of wake effects in the lee of a farm of Wave Dragon wave energy converters. *Renew. Energy*, pp. 1644–1661.

Bejan, A., 2008. *Design with Constructal Theory*. John Wiley & Sons, Hoboken, N.J.

Bejan, A., 2000. *Shape And Structure, From Engineering To Nature*. Cambridge University Press, New York.

Chakrabarti, S.K., 2005. *Handbook of offshore engineering*. Elsevier, Amsterdam; London.

Dos Santos, E.D., Machado, B.N., Zanella, M.M., das Neves Gomes, M., Souza, J.A., Isoldi, L.A., Rocha, L.A.O., 2014. Numerical Study of the Effect of the Relative Depth on the Overtopping Wave Energy Converters According to Constructal Design. *Defect Diffus. Forum*, pp. 232–244.

Falcão, A.F. de O., 2010. Wave energy utilization: A review of the technologies. *Renew. Sustain. Energy Rev.*, pp. 899–918.

FLUENT, 2007. *Documentation Manual – FLUENT 6.3.16*.

Gomes, M. das N., Dos Santos, E.D., Isoldi, L.A., Rocha, L.A.O., 2012. Análise de malhas para geração numérica de ondas em tanques, in: *Proceedings VII Congresso Nacional de Engenharia Mecânica. Presented at the CONEM 2012*, São Luiz - Maranhão.

Goulart, M.M., Martins, J.C., Junior, I.C.A., Gomes, M. das N., Souza, J.A., Rocha, L.A.O., Isoldi, L.A., Santos, E.D. dos, 2015. Constructal design of an onshore overtopping device in real scale for two different depths. *Mar. Syst. Ocean Technol.* 1–10. doi:10.1007/s40868-015-0010-7

Horko, M., 2007. *CFD Optimisation of an Oscillating Water Column Energy Converter*. MSc thesis, The University of Western, School of Mechanical Engineering Faculty of Engineering, Computing and Mathematics.

Iahnke, S.L.P., 2010. *Estado da Arte e Desenvolvimento de um Modelo de Simulação Numérica para o Princípio de Galgamento*. Dissertação de Mestrado em Modelagem Computacional, Universidade Federal do Rio Grande.

Jin, J., Liu, Z., Hong, K., Hyun, B.-S., 2012. 3D Numerical Investigation on Reservoir System for an Overtopping Wave Energy Convertor. *J. Navig. Port Res. Int.*, pp. 97–103.

Kofoed, J.P., 2002. Wave overtopping of marine structures – utilization of wave energy (PhD thesis, Hydraulics & Coastal Engineering Laboratory). Aalborg University, Department of Civil Engineering.

Kofoed, J.P., Frigaard, P., Friis-Madsen, E., Sørensen, H.C., 2006. Prototype testing of the wave energy converter wave dragon. *Renew. Energy*, pp. 181–189.

Liu, Z., Hyun, B., Jin, J., 2008. Numerical Prediction for Overtopping Performance of OWEC. *J. Korean Soc. Mar. Environ. Eng.*, pp. 35–41.

Lv, X., Zou, Q., Reeve, D., 2011. Numerical simulation of overflow at vertical weirs using a hybrid level set/VOF method. *Adv. Water Resour.*, pp. 1320–1334.

Margheritini, L., Stratigaki, V., Troch, P., 2012. Geometry Optimization of an Overtopping Wave Energy Device Implemented into the New Breakwater of the Hanstholm Port Expansion. *Twenty-Second Int. Offshore Polar Eng. Conf.*, pp. 593–600.

Margheritini, L., Vicinanza, D., Frigaard, P., 2009. SSG wave energy converter: Design, reliability and hydraulic performance of an innovative overtopping device. *Renew. Energy*, pp. 1371–1380.

Nam, B.W., Shin, S.H., Hong, K.Y., Hong, S.W., 2008. Numerical Simulation of Wave Flow over the Spiral-Reef Overtopping Device. *The Eighth ISOPE Pacific/Asia Offshore Mechanics Symposium.*, pp. 262-267.

Patankar, S. V., 1980. *Numerical heat transfer and fluid flow*. McGraw Hill, New York, USA.

Rocha, L.A.O., Lorente, S., Bejan, A., 2013. *Constructal Law And The Unifying Principle Of Design*. Springer, New York.

Versteeg, Henk Kaarle, Malalasekera, Weeratunge, 2007. *An Introduction to Computational Fluid Dynamics: The Finite Volume Method*. Pearson.

Zabihian, F., Fung, A.S., 2011. Review of marine renewable energies: Case study of Iran. *Renew. Sustain. Energy Rev*., pp. 2461–2474.

8 RESPONSIBILITY NOTICE

The authors are the only responsible for the printed material included in this paper.